RSC Advances

ROYAL SOCIETY OF CHEMISTRY

www.rsc.org/advances

Triphenylphosphine-assisted highly sensitive fluorescent chemosensor for ratiometric detection of palladium in solution and living cells

Hailiang Nie, Junmin Geng, Jing Jing, Yamin Li, Wen Yang* and Xiaoling Zhang*

Key Laboratory of Cluster Science of Ministry of Education, Beijing Key Laboratory of Photoelectronic/Electrophotonic Conversion Materials, School of Chemistry, Beijing Institute of Technology, 5 Zhongguancun Road, Beijing 100081, P. R. China

E-mail: zhangxl@bit.edu.cn; wenyang@bit.edu.cn;

Fax: +86-10-88875298; Tel: +86-10-88875298.

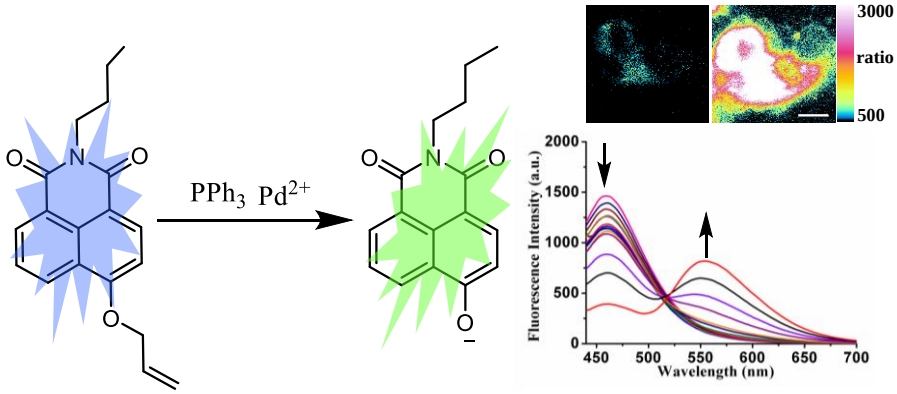

A triphenylphosphine-assisted highly sensitive fluorescent chemosensor for ratiometric detection of palladium in solution and living cells was developed.

RSC Advances

ARTICLE

Triphenylphosphine-assisted highly sensitive fluorescent chemosensor for ratiometric detection of palladium in solution and living cells

Received 00th January 20xx,
Accepted 00th January 20xx

DOI: 10.1039/x0xx00000x

www.rsc.org/

Hailiang Nie, Junming Geng, Jing Jing, Yamin Li, Wen Yang* and Xiaoling Zhang*

Accurate and sensitive detection of palladium (Pd) is essential for both environmental and human health application. This paper describes a triphenylphosphine (PPh_3)-assisted highly sensitive fluorescent chemosensor for ratiometric detection of Pd^{2+} concentrations up to 300 nM with an LOD of 1 nM. During the detection, PPh_3 plays a crucial role in improving the sensitivity of this chemosensor. The chemosensor also has suitable water-solubility which allows detection of Pd^{2+} in solution. Our studies show that it exhibits excellent selectivity toward Pd^{2+} and undergoes a color change from colorless to yellow to allow visual detection of Pd^{2+}. Besides detection in solution, this chemosensor also show great potential as an imaging reagent to detect Pd^{2+} as low as 0.03 ppm in diverse cells.

1. Introduction

Palladium (Pd) detection has received great attention in Chemistry and Biology studies due to the fact that it is a critical material in a variety of industrial application, however, it brings potential harm to the environment and human health. In industry, Pd-derived compounds form efficient universal catalysts,[1-3] which are used on a large scale to promote numerous chemical conversions in the production of fine chemicals, synthetic drugs and polymers.[4,5] Pd metal is an indispensable material in many areas such as automobile catalytic converters, electronics, technology, hydrogen storage, dentistry, jewelry and photography.[6,7] However, Pd-containing substances released from industry can cause serious problems for environment and human health.[8] Current studies indicate Pd can be absorbed by biological materials, and accumulated in the food chain. Once human eats food containing Pd, the heavy metal enters the human body and binds to thiol-containing amino acids, proteins, DNA or other macromolecules.[9,10] The binding to these biological moieties can disturb various physiological processes inside the human body. According to the governmental restrictions, the dietary Pd intake should not exceed than 1.5–15 μg/day per person and the Pd threshold in drugs is 5–10 ppm.[11] In order to have systems help detecting and monitoring the Pd levels, sensitive and accurate method for Pd detection is in great need.

Known for its high sensitivity and specificity, operational simplicity and non-invasive detection, fluorescent chemosensor is particularly preferable for the quantitative or quantitative analysis for environmental and biological samples.[12-15] Using Pd's specific coordination or catalysis reactions as recognition mechanisms,[16] a large number of fluorescent chemosensors have been reported to detect Pd^{2+},[17-29] which is the most abundant existing form of the palladium metal under physiological conditions or in environment. Some of these chemosensors are suitable for measuring Pd^{2+} in biological system.[30-34] However, most of these chemosensors for quantitatively measuring Pd^{2+} concentration are based on fluorescent fluctuation in a single emission channel. The drawback for utilizing single emission channel is that it can bring in uncertainties in detection due to different factors such as variability in chemosensor distribution, instability in the excitation source and effects of the microenvironment.[35-37] In contrast, ratiometric chemosensors can help eliminate some of these uncertainties by introducing the self-calibration mechanism using two emission channels. Though a small number of ratiometric fluorescent chemosensors have been developed, some of them have insufficient soluble in an aqueous medium.[38-41] Additionally, we also noticed among these studies, a high concentration (≥20 μM) of Pd^{2+} are usually used to be incubated with living cells to test the performance of these chemosensor in cellular environment.[30,32-34,42,43] However, the results drawn from these experiments may not directly prove the chemosensor performance in the detection of biological samples containing low levels (e.g. nanomolar level) of Pd^{2+}.

To address these issues, we previously designed a 4-hydroxynaphthalimide-derived ratiometric fluorescent chemodosimeter for imaging palladium in living cells,[43] shown in **scheme 1**. Based on the excellent internal charge transfer (ICT) structure of 4-hydroxynaphthalimide fluorophore,[44,45] the fluorescence wavelength of the chemodosimeter presented a 73 nm redshift after Pd-catalyzed cleavage of propargyl ethers owing to the stronger electron-donating ability of oxygen anion.[46-48] The

Key Laboratory of Cluster Science of Ministry of Education,
Beijing Key Laboratory of Photoelectronic/Electrophotonic Conversion Materials, School of Chemistry, Beijing Institute of Technology,
5 Zhongguancun Road, Beijing 100081, P. R. China
E-mail: zhangxl@bit.edu.cn; wenyang@bit.edu.cn; Fax: +86-10-88875298;
Electronic Supplementary Information (ESI) available: [details of any supplementary information available should be included here]. See DOI: 10.1039/x0xx00000x

chemosensor displayed an appropriate solubility in PBS aqueous solution and high selectivity for Pd detection via measuring fluorescence intensity ratios between the two emission channels (500 nm/558 nm). However, even though the chemodosimeter with

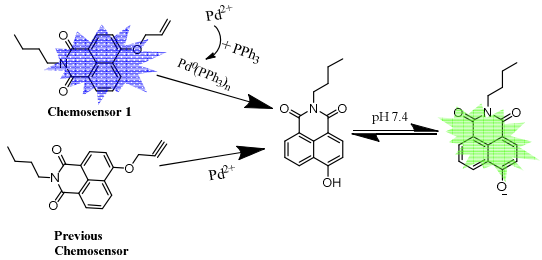

Scheme 1 Proposed recognition mechanisms of chemosensor **1** and previous chemosensor toward Pd^{2+}

a detection limit of 70 nM presented excellent sensitivity for Pd detection in vitro, a high level of Pd^{2+} (40 μM) was still needed to be incubated with cells to perform intracellular imaging experiment. A number of the ratiometric chemosensors that has been reported recently also suffered from the similar problem in high level of Pd^{2+} for incubation.[30,32-34,42,43] These studies indicated that intracellular complex testing conditions might affect the chemosensor sensitivity for Pd^{2+} detection. As a continuation of our previous work, we are dedicated to improve the chemosensor sensitivity for intracellular Pd^{2+} detection. In this work, we developed a high sensitive fluorescent chemosensors **1** for intracellular Pd^{2+} imaging based on triphenylphosphine (PPh_3)-supported Pd-catalyzed deallylation reaction (**Scheme 1**). For the similar chemical structures, chemosensor **1** still maintains the advantages of our previous chemodosimeter including proper aqueous solubility and dual-channel fluorescence emission. However, the detection limit in vitro decreased from 70 nM to 1 nM and the Pd^{2+} concentration used in cell incubation was reduced from 40 μM to 300 nM. The analytical performance of the two chemosensors was compared in table 1 in supporting information. To account for these difference, we found that PPh_3 play a crucial role in improving the sensitivity of chemosensor **1** for Pd^{2+} detection in solution and living cells.

2. Materials and methods

2.1 Materials

The *N*-butyl-4-chloro-1, 8-naphthalimide was synthesized according to our previous work.[49] All other materials were purchased from commercial suppliers and used without further purification. Silica gel (200-300 mesh, Qingdao Haiyang Chemical Co.) was used for column chromatography. ^{1}H NMR spectra were acquired on a Bruker AMX400 spectrometer. Chemical shifts (δ) were reported in ppm relative to a Me_4Si standard. Electrospray ionization (ESI) mass spectra were measured with an LC-MS 2010A (Shimadzu) instrument. Fluorescence measurements were obtained on a Hitachi F-2500 fluorescence spectrometer with a 10 mm quartz cuvette. The pH measurements were made with a Sartorius basic pH-meter PB-10. Confocal imaging was performed in Olympus FV1000-LX81. HPLC was performed on a TechMate C18-ST (5 μM, 4.6 × 250 mm) column (TechMate Technology CO., LTD.) using an HPLC system composed of two pumps (LC-6AD, SHIMADZU) and a detector (SPD-20AV, SHIMADZU).

2.2 Synthetic procedures

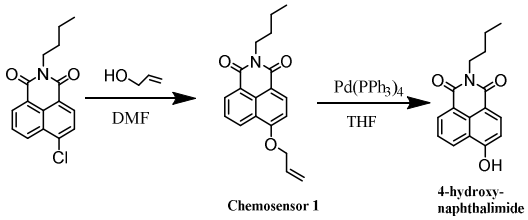

Scheme 2 The synthesis of chemosensor **1** and its Pd^0-catalyzed deallylation product

Chemosensor 1: To a mixture of *N*-butyl-4-chloro-1,8-naphthalimide (863.2 mg, 3 mmol), K_2CO_3 (1.3 g, 10.0 mmol) and 18-crown-6 (30.0 mg, 0.1 mmol) in 10 mL DMF was added allyl alcohol (900.0 mg, 15 mmol). The resulting solution was heated to 100 ºC for 12 h. After cooling to room temperature, the reaction mixture was dropped into 200 mL doubly distilled water. The product was exacted from water using $CHCl_3$ as solvent. After removal of $CHCl_3$, the residues were purified by silica gel column chromatography using $CHCl_3$/petroleum ether (v/v, 1:10) as eluent to afford **1** as a pale yellow solid (431 mg, 46%). ^{1}H-NMR (400 MHz, $CDCl_3$-d_6) δ (*10^{-6}): 0.98 (t, *J* = 7.3 Hz, 3H), 1.42-1.48(m, 2H), 1.68-1.75(m, 2H), 4.17(t, *J* = 7.5 Hz, 2H), 4.85(d, *J* = 5.0 Hz, 2H), 5.42(d, *J* = 10.5 Hz, 1H), 5.55(d, *J* = 17.2 Hz, 1H), 6.14-6.21(m, 1H), 7.03(d, *J* = 8.2 Hz, 1H), 7.26(s, 1H), 7.70(t, *J* = 7.8 Hz, 1H), 8.53(d, *J* = 8.2 Hz, 2H), 8.60(d, *J* = 8.0 Hz, 2H). ^{13}C-NMR (100 MHz, $CDCl_3$-d_6): δ (*10^{-6}): 13.99, 20.56, 30.44, 40.25, 69.73, 106.39, 115.47, 118.85, 122.71, 123.81, 126.08, 128.77, 129.64, 131.68, 132.05, 133.40, 159.80, 164.09, 164.68. ESI -MS calcd for $C_{19}H_{19}NO_3$ $[M+Na]^+$ 332.1, found 332.1.

The reaction product of chemosensor 1 with $Pd(PPh_3)_4$: To a solution of chemosensor **1** (620 mg, 2.00 mmol) in THF (20 mL) was added morpholine (195 mg, 2.20 mmol), sodium borohydride (90.8 mg, 2.40 mmol) and $Pd(PPh_3)_4$ (11.6 mg, 0.01 mmol) at 24 °C. After reaction for 4 h, 3 N HCl (4 mL) was added very slowly to quench the reaction. Then, the solution was extracted with EtOAc, and the organic phase was washed with brine, dried over Na_2SO_4, then filtered and the solvent was evaporated. The residue was purified by silica gel flash chromatography ($CHCl_3$/ petroleum ether, v/v, 1:50) to afford compound **2** as a yellow solid (500 mg, 90%). ^{1}H-NMR (400 MHz, DMSO-d_6) δ (*10^{-6}): 0.85(t, *J* = 6.8 Hz, 3H), 1.23-1.39(m, 2H), 1.56-1.64(m, 2H), 4.03(t, *J* = 7.4 Hz, 2H), 7.16(d, *J* = 8.0 Hz, 1H), 7.75-7.79(m, 1H), 8.35(d, *J* = 1.2 Hz, 1H), 8.37(d, *J* = 1.2 Hz, 1H), 8.48(d, *J* = 7.6 Hz, 1H), 8.54(d, *J* = 8.4 Hz, 1H), 11.85(s, 1H).

^{13}C-NMR (100 MHz, DMSO-d_6): δ (*10^{-6}): 14.12, 20.25, 30.16, 110.31, 113.00, 122.16, 122.73, 125.87, 129.19, 129.51, 131.40, 133.83, 160.60, 163.35, 164.01. HRMS (ESI positive) calcd for $C_{16}H_{15}NO_3$ $[M+H]^+$ 270.11247, found 270.11240.

2.3 Cell culture and Imaging

HepG 2 cells and RAW264.7 macrophage cells (gifted from the center of cells, Institute of Basic Medical Sciences, Chinese Academy of Medical Sciences) were cultured in culture media (DMEM/F12 supplemented with 10% FBS, 1.5 g/L sodium bicarbonate, 1% antibiotics (penicillin /streptomycin, 100 U/ml) at 37 ℃ under a humidified atmosphere containing 5% CO_2. Before use, HepG 2 cells were seeded in a 6-well plate at a density of 10^4 cells per well in culture media. For detecting Pd^{2+}, the cells were incubated with the chemosensor **1** (5 μM) and PPh_3 (4 μM) for 15 min, washed twice with culture media, and observed under confocal fluorescence microscope. Then, the cells were incubated with Pd^{2+} (final concentration: 300 nM) for 15 min and were measured the fluorescence changes. RAW264.7 cells were treated with the same procedures as HepG 2 cells.

3. Results and Discussion

3.1 Spectral response of chemosensor 1 to Pd^{2+} in PPh_3-reducing environment

First, we assessed the catalyzed deallylation reaction between chemosensor **1** and Pd^{2+} in PPh_3-reducing environment. Referring to the previous literatures,[50,51] Pd^{2+} can be reduced to $Pd^0(PPh_3)n$ (n=1~4) in situ by using PPh_3 as a reducing agent and ligand, shown in **Scheme 1.** The generated $Pd^0(PPh_3)n$ catalyzes the allylic oxidative insertion to cleave the allylic C–O bond in chemosensor structures, accompanied by changes in fluorescence signal. Under simulated physiological conditions (PBS solution, 10 mM, pH 7.4), the solution containing chemosensor **1** (5 μM) and PPh_3 (4 μM) exhibited absorption and emission band centered at 375 nm and 460 nm, respectively (**Fig. 1**). Upon an addition of Pd^{2+} (0.5 μM), the maximum absorption peak showed a 75 nm redshift to 450 nm, with the solution color changed from colorless to yellow **(Fig. 1A).** Meanwhile, the maximum emission peak underwent a 100 nm redshift to 560 nm **(Fig. 1B).** These results confirmed that chemosensor **1** could serve as a naked-eye and ratiometric indicator for Pd^{2+} detection in solution.

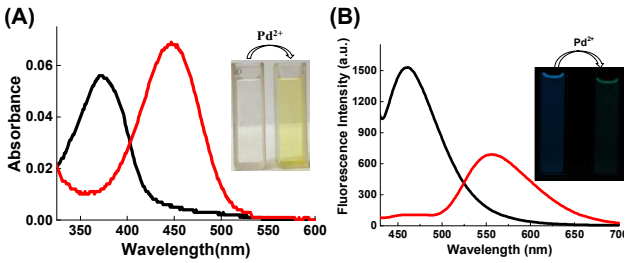

Figure 1 (A) Absorption spectra and **(B)** fluorescence spectra of chemosensor **1** (5 μM, containing 4 μM PPh_3) before and after addition of Pd^{2+} (0.5 μM), measured in PBS buffer (10 mM, pH 7.4). The blank line is for chemosensor **1** and the red line is for chemosensor **1** + Pd^{2+}. Inserts show the changes of the color and fluorescence of the solution before and after addition of Pd^{2+}. Each spectrum was acquired after Pd^{2+} addition for 1 h at room temperature. λ_{ex}= 410 nm.

To confirm the mechanism of chemosensor 1 in sensing Pd^{2+}, the reaction process was monitored by high phase liquid chromatography (HPLC). As shown in **Fig.S1**, in PBS solution (pH=7.4), chemosensor 1 can converted into 4-hydroxy-naphthalimide in the presence of $PdCl_2$ and PPh_3 **(Fig. S1C).** However, in THF medium (see **Synthetic procedures**), the deallylation reaction can be hardly performed in the presence of $Pd(PPh_3)_4$ **(Fig. S1A)**. To enhance turnover, $NaBH_4$ was chosen as a reducing agent because of its known ability to efficiently reduce Pd^{2+} to Pd^0.[50] The result showed that $NaBH_4$ significantly enhanced the Pd-catalyzed deallylation of chemosensor 1 in THF medium **(Fig. S1B)**.

3.2 The effect of PPh_3 on the recognition reaction

Next, we examined the effect of PPh_3 on the recognition reaction. As seen in **Fig. 2,** the fluorescence spectral of chemosensor **1** (5 μM) presented limited change in the presence of Pd^{2+} (0.5 μM), indicating the deallylation reaction is hardly performed under Pd^{2+} catalysis. Chemosensor **1** showed almost the same fluorescence spectra in the absence and presence of PPh_3 (4 μM), confirming that PPh_3 itself does not affect the chemosensor emission spectra. Additionally, PPh_3 and $Pd(PPh_3)_4$ show no fluorescence emission in detection wavelength range. The fluorescence spectral only underwent a large redshift in both presence of PPh_3 and Pd^{2+}. These results revealed that PPh_3 plays a crucial role in recognition reaction. According to the previous study by Koide's group,[50,51] Pd^{2+} can be converted to $Pd^0(PPh_3)n$ in PPh_3-reducing environment. As a result, we achieved the same conversion in the chemosensor spectral when $Pd(PPh_3)_4$ was used in lieu of $PdCl_2$ and PPh_3 (**Fig. 2**). Moreover, in PPh_3-reducing environment, an optimal time for the reaction between chemosensor **1** and Pd^{2+} was between 60 to 90 min (**Fig. S2**).

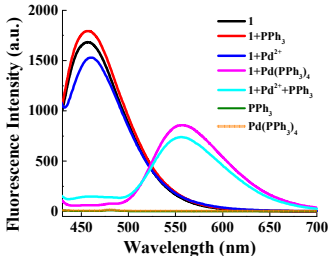

Figure 2 Fluorescence response of chemosensor 1 (5 μM) toward PPh_3 (4 μM), Pd^{2+} (0.5 μM), $Pd(PPh_3)_4$ (0.5 μM), PPh_3 (4 μM) + Pd^{2+} (0.5 μM), respectively, and the fluorescence spectral of PPh_3 (4 μM) and $Pd(PPh_3)_4$ (0.5 μM) in wavelength range of 430~700 nm. All experiments were performed in PBS buffer (10 mM, pH 7.4). λ_{ex}= 410 nm.

3.3 Sensitivity of chemosensor 1 toward Pd^{2+}

Chemosensor **1** showed high sensitivity for ratiometric detection of Pd^{2+} in PBS solution (10 mM, pH 7.4). As seen in **Fig. 3**, upon an increasing addition of Pd^{2+} (final concentration: 0~250 nM), the solution containing chemosensor **1** (5 μM) and PPh_3 (4 μM) presented a gradual decrease in fluorescent intensity at 460 nm, with a corresponding increase at 560 nm. In addition, a well-defined isoemission point at around 517 nm was also observed, indicating that a new species was formed. The logarithm of the fluorescence intensity ratio at two emission peaks, $\log(F_{560}/F_{460})$, changed from -1.1 to 0.31 after addition of Pd^{2+} (250 nM). There was a good linearity (R^2=0.990) between $\log(F_{560}/F_{460})$ and Pd^{2+} concentrations in the range of 20~250 nM **(Fig, 2)**. The detection limit of chemosensor **1** is 1 nM **(see supporting information)**, to our knowledge, this value is the lowest in reported ratiometric chemosensors for measuring Pd^{2+}.

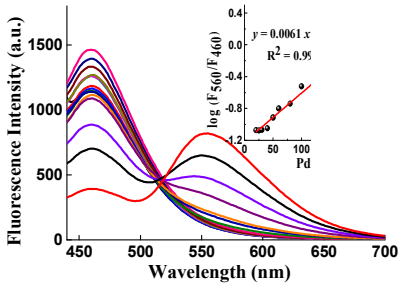

Figure 3 Fluorescence responses of chemosensor **1** (5 μM, contaiing 4 μM PPh_3) toward Pd^{2+} (final concentration: 0, 4, 8, 10, 15, 20, 25, 30, 40, 50, 60, 80, 100, 150, 200, 250 nM). Insert: the linear relatiomship between $\log(F_{560}/F_{460})$ and Pd^{2+} concentrations. All experiments were performed after reacting with metal ions for 1 h in PBS solution (10 mM, pH=7.4). λ_{ex} = 410 nm.

3.4 Selectivity of chemosensor 1 toward Pd^{2+}

The selectivity of chemosensor **1** toward various metal ions was also investigated. Under the same conditions (10 mM PBS, pH

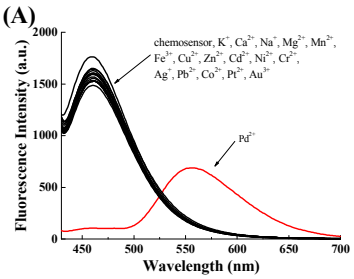

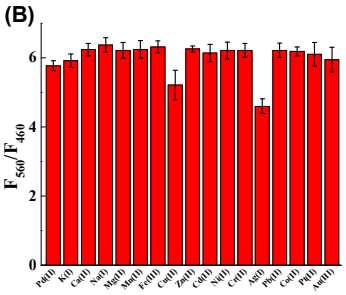

Figure 4 (A) Fluorescence responses of chemosensor 1 (5 μM, containing 4 μM PPh_3) toward various metal ions (0.5 μM for Pd^{2+}, 3 μM for other ions). (B) Fluorescence responses of chemosensor 1 (5 μM, containing 4 μM PPh_3) toward Pd^{2+} (0.5 μM) in the presence of various metal ions (3 μM for other ions). All experiments were performed after reacting with metal ions for 1 h in PBS solution (10 mM, pH=7.4). λ_{ex} = 410 nm.

7.4), chemosensor **1** exhibited no apparent fluorescence change in the presence of other metal ions, even other π-philic metals such as Ag, Ni, Au, Co, Hg (**Fig. 4A**). Moreover, the interference of the above-mentioned metal ions on monitoring Pd were also studied (**Fig. 4B**). These results showed chemosensor **1** possesses high selectivity toward Pd^{2+} even in the presence of other metal ions.

3.5 Ratiometric imaging of Pd^{2+} in living cells

To further demonstrate the practical application of chemosensor **1** in living systems**,** the experiments were carried out in HepG2 and RAW 264.7 macrophage cells. As seen in **Fig. 5**, the cells incubated with chemosensor **1** (5 μM) and PPh_3 (4 μM) for 15 min showed an intense intracellular fluorescence, indicating that chemosensor **1** could penetrate cell membranes. Then, upon addition of Pd^{2+} (300 nM, equivalent to 0.03 ppm), the fluorescence intensity ratios at two emission channels increased immediately (**Fig. 5c**). These results demonstrate that the cellular uptake of Pd^{2+} as low as 0.03 ppm, which is substantially lower than the specified threshold in drugs (5–10 ppm), could be determined by using chemosensor **1** as an imaging reagent. Moreover, the RAW 264.7 cells showed a similar phenomenon in dual emission channels under stimulation of Pd^{2+} **(Fig. 6)**, indicated that chemosensor **1** can be used for Pd^{2+} detection in diverse cells.

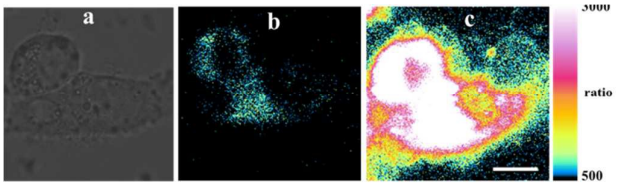

Figure 5 Ratiometric imaging of Pd^{2+} in living HepG 2 cells by using confocal fluorescence microscope. The cells were incubated with chemosensor **1** (5 μM) and PPh_3 (4 μM) for 15 min: **(a)** the bright-field transmission image; **(b)** the ratio images generated from green channel at 515±30 nm and blue channel at 450±35 nm. Then, the cells were incubated with Pd^{2+} (300 nM) for 15 min: **(c)** the ratio images generated from green channel at 515±30 nm and blue channel at 450±35 nm. Incubation was performed at 37 °C under a humidified atmosphere containing 5% CO_2. Scale bar = 10 μm.

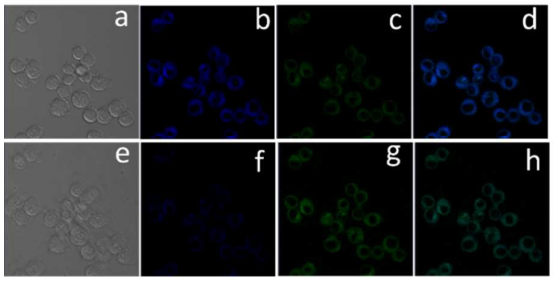

Figure 6 Fluorescence imaging of Pd^{2+} in RAW 264.7 macrophage cells. The cells were incubated with chemosensor **1** (5 μM) and PPh_3 (4 μM) for 15 min: **(a)** bright-field image, **(b)** blue channel at 450±35 nm, **(c)** green channel at at 515±30 nm, and **(d)** mixed image generated from **(c)** and **(b).** Then, the cells were incubated with Pd^{2+} (300 nM) for 15 min: **(e)** bright-field image, **(f)** blue channel at 450±35 nm, **(g)** green channel at at 515±30 nm, and **(h)** mixed image generated from **(f)** and **(g)**. Incubation was performed at 37 °C under a humidified atmosphere containing 5% CO_2.

To estimate the cytotoxicity of chemosensor **1**, we performed 3-(4,5-dimethylthiazol-2-yl)-2,5-diphenyltetrazolium bromide (MTT) assays in RAW 264.7 cells with 5, 10 and 20 μM chemosensor **1** (containing 4 μM PPh_3) for 24 h, respectively. The experimental results in **Fig. S3**, showed that our probe exhibited very low toxicity to cultured cells at a concentration of 5 μM in the experimental conditions.

Conclusions

In conclusion, we have developed a highly sensitive 4-hydroxynaphthalimide-derived fluorescent chemosensor **1** for ratiometric detection of Pd^{2+} in PPh_3-reducing environment. Chemosensor **1** can detect Pd^{2+} quantitatively by ratiometric fluorescence method with a 100 nm red-shifted emission wavelength in the concentration up to 300 nM with a detection limit of 1 nM. During the detection, PPh_3 play a crucial role in improving the chemosensor sensitivity. The chemosensor also has suitable water-solubility, exhibits excellent selectivity toward Pd^{2+}, and undergoes a color change from colorless to yellow for "naked eye" detection of Pd^{2+}. Finally, we demonstrated that chemosensor **1** can be used as an imaging reagent to detect Pd^{2+} as low as 0.03 ppm in diverse cells.

Acknowledgements

This work was financially supported by the National Nature Science Foundation of China (No. 21275018, 21575015 and 21203008), Beijing National Laboratory for Molecular Sciences (BNLMS) **(**20140121**),** Research Fund for the Doctoral Program of Higher Education of China (RFDP) (No. 20121101110049) and the 111 Project (B07012) for financial support.

References

1 C. Xu, L. Deiana, S. Afewerki, C. Incerti-Pradillos, O. Cordova, P. Guo, A. Cordova and N. Hedin, *ADV SYNTH CATAL*, 2015, **357**, 2150-2156.
2 X. Wu, H. Neumann and M. Beller, *CHEM REV*, 2013, **113**, 1-35.
3 G. Zeni and R. C. Larock, *CHEM REV*, 2004, **104**, 2285-2309.
4 S. L. Buchwald, C. Mauger, G. Mignani and U. Scholz, *ADV SYNTH CATAL*, 2006, **348**, 23-39.
5 C. E. Garrett and K. Prasad, *ADV SYNTH CATAL*, 2004, **346**, 889-900.
6 R. Rushforth, *PLATIN MET REV*, 2004, **48**, 30-31.
7 W. Grochala and P. P. Edwards, *CHEM REV*, 2004, **104**, 1283-1315.
8 S. Zimmermann, F. Alt, J. Messerschmidt, A. von Bohlen, H. Taraschewski and B. Sures, *ENVIRON TOXICOL CHEM*, 2002, **21**, 2713-2718.
9 International Program on Chemical Safety, Palladium, Environmental Health Criteria Series 226, World Health Organization, Geneva, 2002.
10 J. Kielhorn, C. Melber, D. Keller and I. Mangelsdorf, *INT J HYG ENVIR HEAL*, 2002, **205**, 417-432.
11 C. E. Garrett and K. Prasad, *ADV SYNTH CATAL*, 2004, **346**, 889-900.
12 Z. Guo, S. Park, J. Yoon and I. Shin, *CHEM SOC REV*, 2014, **43**, 16-29.
13 X. Li, X. Gao, W. Shi and H. Ma, *CHEM REV*, 2014, **114**, 590-659.
14 H. N. Kim, Z. Guo, W. Zhu, J. Yoon and H. Tian, *CHEM SOC REV*, 2011, **40**, 79-93.
15 Y. Sun, J. Liu, X. Lv, Y. Liu, Y. Zhao and W. Guo, *ANGEW CHEM INT EDIT*, 2012, **51**, 7634-7636.
16 H. Li, J. Fan and X. Peng, *CHEM SOC REV*, 2013, **42**, 7943-7962.
17 M. Wang, X. Liu, H. Lu, H. Wang and Z. Qin, *ACS APPL MATER INTER*, 2015, **7**, 1284-1289.
18 A. K. Mahapatra, S. K. Manna, K. Maiti, S. Mondal, R. Maji, D. Mandal, S. Mandal, M. R. Uddin, S. Goswami, C. K. Quah and H. Fun, *ANALYST*, 2015, **140**, 1229-1236.
19 R. Zhang, M. Gao, S. Bai and B. Liu, *J MATER CHEM B*, 2015, **3**, 1590-1596.
20 W. R. Kitley, P. J. Santa Maria, R. A. Cloyd and L. M. Wysocki, *CHEM COMMUN*, 2015, **51**, 8520-8523.
21 J. Cui, D. Li, S. Shen, J. Liu and B. Zhao, *RSC ADV*, 2015, **5**, 3875-3880.
22 H. Wang, Y. Lang, H. Wang, J. Lou, H. Guo and X. Li, *TETRAHEDRON*, 2014, **70**, 1997-2002.
23 D. Keum, S. Kim and Y. Kim, *CHEM COMMUN*, 2014, **50**, 1268-1270.
24 A. Kumar, M. Chhatwal, A. K. Singh, V. Singh and M. Trivedi, *CHEM COMMUN*, 2014, **50**, 8488.
25 Z. Wang, S. Zheng, J. Cai, P. Wang, J. Feng, X. Yang, L. Zhang, M. Ji, F. Wu, N. He and N. Wan, *ANAL CHEM*, 2013, **85**, 11602-11609.
26 J. M. Williams and K. Koide, *IND ENG CHEM RES*, 2013, **52**, 8612-8615.
27 J. He, M. Zha, J. Cui, M. Zeller, A. D. Hunter, S. Yiu, S. Lee and Z. Xu, *J AM CHEM SOC*, 2013, **135**, 7807-7810.
28 H. Li, J. Fan, J. Du, K. Guo, S. Sun, X. Liu and X. Peng, *CHEM COMMUN*, 2010, **46**, 1079-1081.
29 L. Duan, Y. Xu and X. Qian, *CHEM COMMUN*, 2008, 6339.
30 H. Cui, H. Chen, Y. Pan and W. Lin, *Sensors and Actuators B: Chemical*, 2015, **219**, 232-237.
31 U. Reddy G., F. Ali, N. Taye, S. Chattopadhyay and A. Das, *CHEM COMMUN*, 2015, **51**, 3649-3652.
32 M. Yang, Y. Bai, W. Meng, Z. Cheng, N. Su and B. Yang, *INORG CHEM COMMUN*, 2014, **46**, 310-314.
33 J. Hou, K. Li, K. Yu, M. Ao, X. Wang and X. Yu, *The Analyst*, 2013, **138**, 6632.
34 M. Santra, S. Ko, I. Shin and K. H. Ahn, *CHEM COMMUN*, 2010, **46**, 3964.

35 L. Yuan, W. Lin, K. Zheng and S. Zhu, *ACCOUNTS CHEM RES*, 2013, **46**, 1462-1473.
36 W. Niu, L. Fan, M. Nan, Z. Li, D. Lu, M. S. Wong, S. Shuang and C. Dong, *ANAL CHEM*, 2015, **87**, 2788-2793.
37 Y. Han, C. Ding, J. Zhou and Y. Tian, *ANAL CHEM*, 2015, **87**, 5333-5339.
38 X. Chen, H. Li, L. Jin and B. Yin, *TETRAHEDRON LETT*, 2014, **55**, 2537-2540.
39 X. Wang, Z. Guo, S. Zhu, H. Tian and W. Zhu, *CHEM COMMUN*, 2014, **50**, 13525-13528.
40 S. Sun, B. Qiao, N. Jiang, J. Wang, S. Zhang and X. Peng, *ORG LETT*, 2014, **16**, 1132-1135.
41 J. Jiang, H. Jiang, W. Liu, X. Tang, X. Zhou, W. Liu and R. Liu, *ORG LETT*, 2011, **13**, 4922-4925.
42 W. Liu, J. Jiang, C. Chen, X. Tang, J. Shi, P. Zhang, K. Zhang, Z. Li, W. Dou, L. Yang and W. Liu, *INORG CHEM*, 2014, **53**, 12590-12594.
43 B. Zhu, C. Gao, Y. Zhao, C. Liu, Y. Li, Q. Wei, Z. Ma, B. Du and X. Zhang, *CHEM COMMUN*, 2011, **47**, 8656-8658.
44 R. M. Duke, E. B. Veale, F. M. Pfeffer, P. E. Kruger and T. Gunnlaugsson, *CHEM SOC REV*, 2010, **39**, 3936-3953.
45 P. Jin, C. Jiao, Z. Guo, Y. He, S. Zhu, H. Tian and W. Zhu, *CHEM SCI*, 2014, **5**, 4012-4016.
46 B. Zhu, B. Guo, Y. Zhao, B. Zhang and B. Du, *BIOSENS BIOELECTRON*, 2014, **55**, 72-75.
47 C. Liu, H. Wu, Z. Wang, C. Shao, B. Zhu and X. Zhang, *CHEM COMMUN*, 2014, **50**, 6013-6016.
48 F. Song, S. Watanabe, P. E. Floreancig and K. Koide, *J AM CHEM SOC*, 2008, **130**, 16460-16461.
49 S. Zhang, J. Geng, W. Yang and X. Zhang, *RSC ADV*, 2014, **4**, 12596-12600.
50 A. L. Garner, F. Song and K. Koide, *J AM CHEM SOC*, 2009, **131**, 5163-5171.
51 F. Song, A. L. Garner and K. Koide, J AM CHEM SOC, 2007, 129, 12354-12355.